

# Triplet-State Properties and Singlet Oxygen Generation in a Homologous Series of Functionalized Fullerene Derivatives

Ferran Prat, Robert Stackow, Robert Bernstein, Wenyuan Qian, Yves Rubin, and Christopher S. Foote\*

Department of Chemistry and Biochemistry, University of California, Los Angeles, California 90095-1569

Received: April 15, 1999; In Final Form: June 14, 1999

The main properties of the triplet states and the yields of singlet oxygen generation for a series of methano-[60]fullerene adducts with increasing numbers of substituents were determined. The triplet properties investigated are energies, triplet–triplet absorption spectra, extinction coefficients, and quantum yields. A strong correlation is observed between several triplet properties and the topology of the fullerene core. Successive fragmentation of the chromophore of the parent C<sub>60</sub> results in higher triplet energies and lower triplet quantum yields. In addition, singlet oxygen quantum yields ( $\phi_{\Delta}$ ) were determined for all adducts and decrease as the area of the conjugated fullerene core decreases.

## Introduction

Since their initial synthesis, the photophysical properties of fullerene adducts have attracted much attention.<sup>1–9</sup> Functionalization of fullerenes allows them to be used in a variety of applications. However, this alteration can modify properties that make fullerenes interesting from a photophysical standpoint. Extensive research has been devoted to several of these derivatives, with special emphasis on methano- and pyrrolidino-[60]fullerene derivatives, mainly because of their ease of synthesis.<sup>10–12</sup> While a wealth of information is now available for monoadducts, little is known about multiply functionalized fullerenes, with the exception of selected photophysical and redox properties.<sup>4,8,9,13,14d–g</sup> Most reports agree that perturbation of the fullerene  $\pi$  system results in a substantial change in photophysical properties. Similar effects are observed in electrochemistry: first reduction potentials become increasingly negative with lower degrees of conjugation.<sup>13</sup> The triplet states of these compounds have not been thoroughly investigated, and a clear relationship between structure and triplet properties has not yet been established.<sup>9</sup>

The triplet quantum yield ( $\phi_T$ ) is near unity for C<sub>60</sub>.<sup>15</sup> Previous studies point to a substantial decrease in triplet quantum yield upon interruption of the fullerene core.<sup>1,16</sup> This study aims to clarify the relationship between fullerene structure and triplet properties by analyzing a complete homologous series of fullerene adducts. This series comprises the parent compound C<sub>60</sub> and adducts formed by successive regioselective additions of dialkylmalonate (“Bingel adducts”), with one to six addends attached to the C<sub>60</sub> molecule at pseudo-octahedral sites. Each addition causes a [6,6] double bond in the original fullerene core to be replaced by an annulated cyclopropane, resulting in successively smaller conjugated area. However, the conjugation is not removed completely, since the cyclopropane ring is capable of some homoconjugation; thus, these adducts are not expected to behave identically to other fullerene adducts without cyclopropane rings.<sup>17</sup> Analysis of the change in photophysical properties for this series should provide a greater understanding of the relationship between the fullerene structure and its excited-state properties.

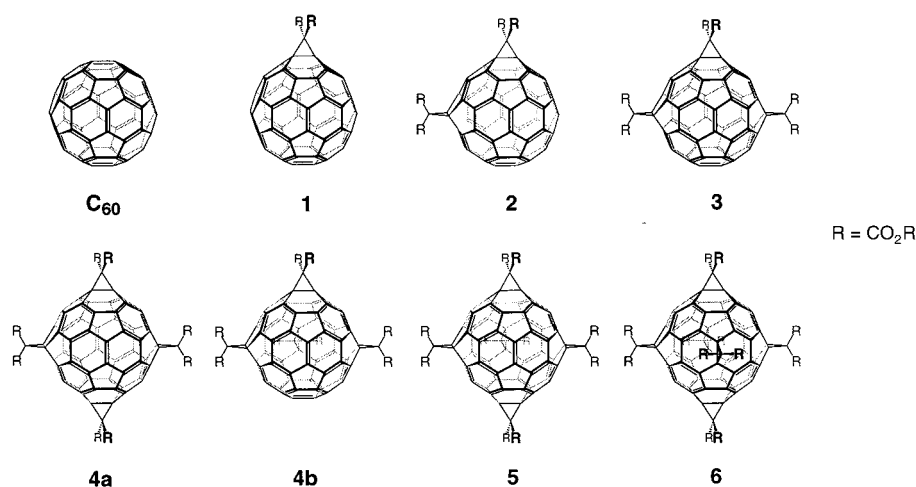
## Experimental Section

**Materials.** Samples of this series of methano derivatives (see Scheme 1) were synthesized by a tether-directed functionalization strategy to be published elsewhere.<sup>14,18</sup> The members of the series are: C<sub>60</sub> (buckminsterfullerene), (1) C<sub>60</sub>[C(COOEt)<sub>2</sub>], (2) *e*-C<sub>60</sub>[C(COOMe)<sub>2</sub>]<sub>2</sub>, (3) *e*-face, *e*-edge, *trans*-1-C<sub>60</sub>-[C(COOMe)<sub>2</sub>]<sub>3</sub>, (4a) *D*<sub>2h</sub>-all-*e*-C<sub>60</sub>[C(COOEt)<sub>2</sub>]<sub>4</sub>, (4b) *C*<sub>s</sub>-all-*e*-C<sub>60</sub>[C(COOMe)<sub>2</sub>]<sub>4</sub>, (5) all-*e*-C<sub>60</sub>[C(COOMe)<sub>2</sub>]<sub>5</sub>, (6) *T*<sub>h</sub>-all-*e*-C<sub>60</sub>[C(COOEt)<sub>2</sub>]<sub>6</sub>. C<sub>60</sub> (purity > 99.5%) was obtained from MER Corp.<sup>19</sup> Rubrene, benzo[*a*]pyrene, anthracene, and ferrocene were used as purchased from Aldrich. Toluene (Optical Grade) and iodoethane were purchased from Aldrich. Methylcyclohexane and 2-methyltetrahydrofuran were purchased from Fisher and used as received.

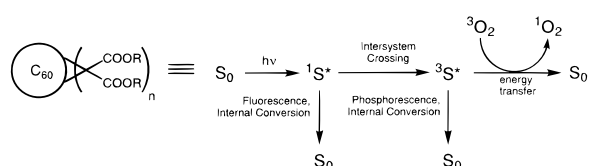
**Measurements.** UV–vis absorption spectra were recorded using a Beckman DU-650 spectrophotometer. Phosphorescence spectra were recorded using a SPEX-Fluorolog 2 spectrometer equipped with a Hamamatsu R928 photomultiplier and a 1943D phosphorimeter in front-face mode using a flash lamp with 10  $\mu$ s pulses.<sup>20</sup> These measurements were carried out at 77 K in a mixture of 2:1:1 methylcyclohexane/2-methyltetrahydrofuran/iodoethane (HFI) as the glass-forming solvent.<sup>9,21</sup> The excitation and emission slits were 8 and 2 mm, respectively. The signal at each wavelength was the average of at least 200 flashes, and the final spectrum for each compound is the average of at least five successive spectra. Triplet energies were calculated from the initial onset of the observed phosphorescence bands.<sup>21</sup>

Triplet–triplet spectra, triplet–triplet extinction coefficients, triplet quantum yields, and triplet energies (using energy transfer) were determined using a transient absorption setup described previously.<sup>22</sup> The excitation light source is a Quanta-Ray DCR-2 Nd:YAG laser providing 532 or 355 nm pulses of 6–7 ns width. A 75 W xenon arc lamp (Photon Technology International) is used for the monitoring beam. Detection of the signal in the visible region was performed with a Hamamatsu R928 photomultiplier tube. The excitation wavelength for all triplet–triplet transient absorption experiments was 355 nm. Samples of  $A_{355} \approx 0.4$  in toluene were placed in a 1 cm quartz cuvette and purged with argon for 30 min. Data were collected

## SCHEME 1



## SCHEME 2



by a Macintosh Iicx using LabView 2 software and analyzed using Igor Pro 3.13.

Energy-transfer experiments to observe quenching of the triplet state of fullerene adduct **2** were accomplished via the transient absorption methods described above. The adduct was dissolved in toluene ( $A_{355} \approx 0.4$ ) and deaerated under argon for 30 min and the selected quencher added. Adduct **2** was excited at 355 nm for energy transfer to benzo[*a*]pyrene and ferrocene and at 532 nm for anthracene. The triplet decay was recorded at the  $\lambda_{\text{max}}$  of the triplet-triplet spectrum of **2**, 710 nm, and the rate constant of quenching was extracted using curve-fitting analysis. Detection of the  $\text{C}_{60}^{\bullet-}$  was performed using the same transient absorption setup as described before. Detection was performed with an Applied Detectors ADC403HS nitrogen-cooled reverse-bias germanium photodiode suitable for use in the near-IR portion of the spectrum.

Singlet oxygen quantum yields were determined by using the Ge photodiode to observe the 1268 nm emission of  $^1\text{O}_2$ . Air-saturated toluene samples were excited at 355 nm. A silicon cutoff filter at 1100 nm and a 1270 nm interference filter were used to eliminate the fluorescence from the sample and scattered laser light. Collection of the data was done at a  $90^\circ$  angle to the laser beam and was enhanced by addition of a parabolic mirror at a  $270^\circ$  angle. Data were collected as described above.

The stability of the fullerene adducts with respect to irradiation was tested. Samples were irradiated in a water bath maintained at room temperature using a 300 W xenon lamp. Mono- and tris-adducts showed no change when monitored by HPLC analysis under air. Mono- and bis-adducts showed no change under an argon atmosphere. The fullerene adducts appear stable to the experimental conditions.

## Results and Discussion

The compounds used are shown in Scheme 1. The photo-physical processes studied are summarized in Scheme 2. Since the malonate moieties are unreactive under the given conditions, within this series all photophysical properties are attributed to the fullerene core.<sup>9,16</sup>

**Ground-State Absorption.** Although the UV-vis spectra of the compounds under study are not directly related to the triplet state, and some have been published elsewhere,<sup>14d</sup> they are included for completeness and are shown in Figure 1. In all cases, the spectra agree with those that have been published. The shapes of the spectra for the eight fullerenes suggest significant and progressive changes in the chromophores depending on the number of addends. Generally, successive additions of malonate moieties result in the disappearance of the longer wavelength bands in the visible portion of the spectrum, as expected because of the smaller conjugated area of the products.<sup>14d</sup> Unlike non-cyclopropane monoadducts, the Bingel adducts lack the weak band just above 700 nm.<sup>2,3</sup> The first observable result of functionalization of the fullerene is the loss of the valley at 435 nm. The two tetra-adducts **4a** and **4b** show very different spectra, presumably as a result of the different geometries of the fullerene core. Whereas **4a** presents a larger fused area divided into two tetrabenzopyraclylene portions (vide infra), **4b** has a smaller, contiguous, fused area. This may account for the fact that **4b** absorbs at longer wavelengths than **4a**. Compounds **5** and **6** show only weak end-absorption in the visible portion of the spectrum.

**Triplet Energies.** The energies of the triplet states of the fullerenes were calculated from the onset of the shortest wavelength peak of the phosphorescence spectra (Figure 2). It was necessary to use a heavy-atom solvent glass at 77 K in order to detect significant phosphorescence from any of the compounds.<sup>21</sup> The majority of the compounds showed very weak phosphorescence in the visible or near-IR except for **1** and **4b**, for which no signal could be detected. The calculated triplet energies are shown in Table 1.

A previous study on *cis*, equatorial, and *trans* adducts reported the phosphorescence of the fullerene derivatives to be independent of the functionalization, showing a single peak at ca. 825 nm, regardless of the number or orientation of the substituents.<sup>9</sup> This signal could not be observed because of the limitations of our apparatus, whose sensitivity drops off dramatically after 800–820 nm.

In our experiments with different (predominantly equatorial) adducts, we observed that the degree of substitution has a substantial effect on the energy of the triplet. The calculated triplet energies show a strong correlation with the conjugated fused area of the fullerene core (Figure 3). Total conjugated fused area was calculated by the summation of the areas of the remaining fused hexagons and pentagons in the fullerene derivative core by simple geometry. This trend is apparent not

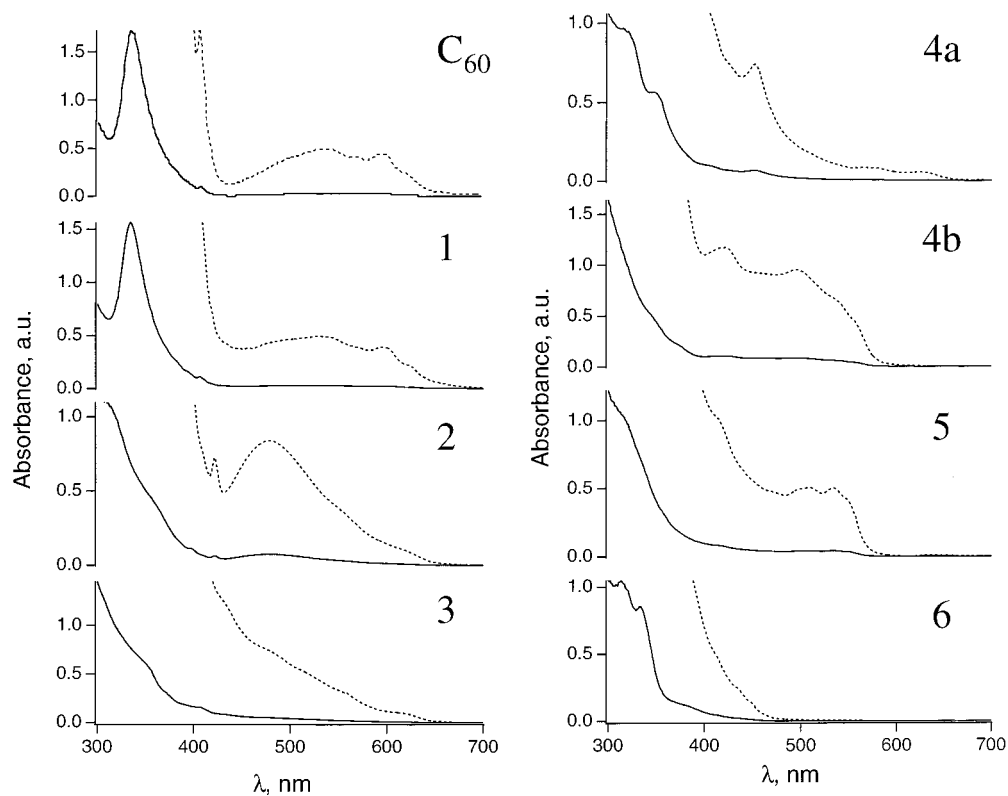


**Figure 1.** UV-vis spectra of the complete series. Dashed lines are  $\times 10$  except for  $C_{60}$  and **1**, which are  $\times 15$ .

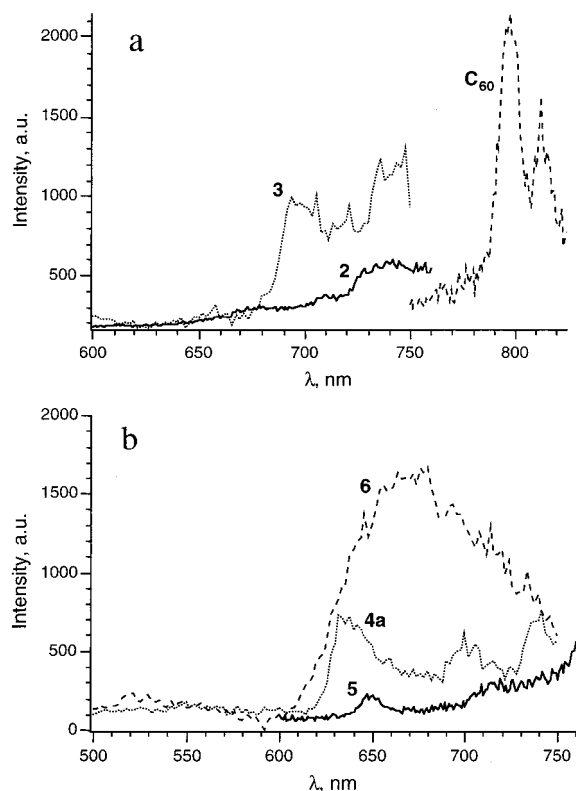


**Figure 2.** Phosphorescence spectra in 2:1:1 methylcyclohexane/2-methyltetrahydrofuran/iodoethane (HFI) at 77 K in front-face mode using a flash lamp with 10  $\mu$ s pulses followed by a 10  $\mu$ s delay. The excitation and emission slits were 8 and 2 mm, respectively.

only for the triplet energies but also for most other triplet state properties, as will be discussed later.

Several controls were performed to confirm the triplet energies. The solvent used, HFI, has been shown to completely

**TABLE 1:  $E_T$  for Fullerene Derivatives in HFI at 77 K Obtained from Onsets of Absorptions Shown in Figure 2**

compound	onset, nm	$E_T$ , kcal/mol
$C_{60}$	780 <sup>a</sup>	36.7 <sup>a</sup>
<b>1</b>	800 <sup>b</sup>	35.7 <sup>b</sup>
<b>2</b>	710	40.3
<b>3</b>	675	42.4
<b>4a</b>	615	46.5
<b>4b</b>	<sup>c</sup>	
<b>5</b>	640	44.7
<b>6</b>	605	47.3

<sup>a</sup> An identical value was observed by Zeng et al.<sup>21</sup> <sup>b</sup> Calculated from the data published by Asmus et al. and by Williams et al.<sup>6,9</sup> <sup>c</sup> Not observed.

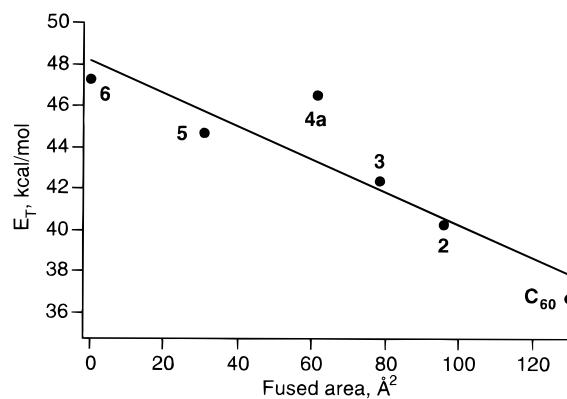


**Figure 3.** Energies of the triplet states observed experimentally as a function of the fused area of the fullerene core.

eliminate the fluorescence of  $C_{60}$  and monoadducts.<sup>9,21</sup> Also, a pulsed lamp was used to excite the fullerenes, and a variable delay was introduced between the pulse and the start of the signal acquisition to eliminate any residual fluorescence. In all cases, increasing the delay resulted in a decrease of the signal

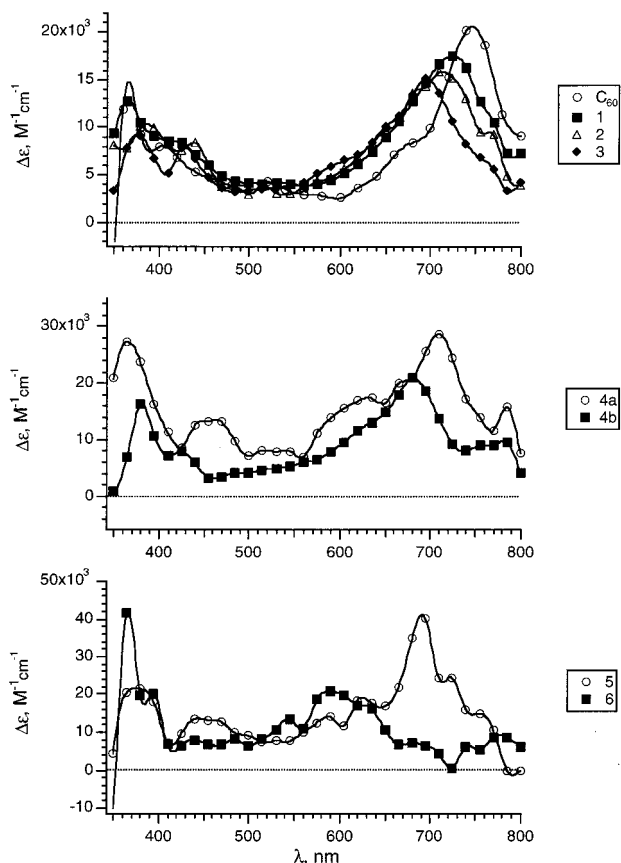


**Figure 4.** Triplet-triplet absorption spectra. All samples ( $A \approx 0.4$ ) were purged with argon for 30 min and excited at 355 nm. Spectra were not corrected for ground-state depletion.

**TABLE 2: Extinction Coefficients and Triplet Quantum Yields in Toluene**

compound	$\Delta\epsilon_{T-T}$ , $\text{M}^{-1} \text{cm}^{-1}$	$\lambda(\text{max})$ , nm	$\phi_T$
$\text{C}_{60}$	20 200 <sup>29</sup>	750	1
<b>1</b>	17 496	725	0.95
<b>2</b>	15 807	710	0.79
<b>3</b>	15 085	695	0.69
<b>4a</b>	20 914	680	0.42
<b>4b</b>	28 762	710	0.20
<b>5</b>	40 042	695	0.07
<b>6</b>	20 871	590	0.11

intensity, but identical spectra. Luminescence due to delayed fluorescence cannot be ruled out; however, this phenomenon was not observed for  $\text{C}_{60}$  with this experimental setup. Finally, a series of energy-transfer experiments using transient absorption were performed with compound **2** to determine its triplet energy unambiguously, since its phosphorescence spectrum is more complex than that of the other compounds.

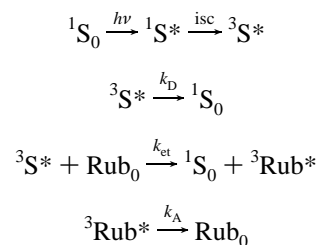
Anthracene and benzo[*a*]pyrene, with triplet energies of 42.5 and 41.8 kcal/mol,<sup>23</sup> did not quench the triplet state of **2**, whereas ferrocene ( $E_T = 37.9$  kcal/mol)<sup>23</sup> quenched it with an approximate rate constant of  $k_q = 8 \times 10^9 \text{ M}^{-1} \text{ s}^{-1}$ . This energy transfer was observed as a quenching of the triplet lifetime of the fullerene adduct using the transient absorption setup described earlier. Subsequent curve-fitting analysis of the data yielded the rate constants associated with observed energy transfer. Ferrocene has been shown to quench the triplet state of polycyclic aromatic compounds by energy transfer as the sole mechanism.<sup>24</sup> Toluene was chosen as the solvent in order to avoid possible competing electron transfer. To further confirm the absence of electron transfer from ferrocene to **2**, flash photolysis experiments were conducted between ferrocene and

$\text{C}_{60}$ , which is more easily reduced than the other adducts.<sup>1</sup> Ferrocene quenches the triplet state of  $\text{C}_{60}$  but does not produce  $\text{C}_{60}^{\bullet-}$ , as indicated by the absence of the 1070 nm transient absorption corresponding to the maximum of the fullerene anion absorption.<sup>25</sup> Formation of a contact ion pair not leading to dissociation cannot be ruled out, and therefore, this experiment is not conclusive. However, the weight of this combined evidence suggests that the onset of the phosphorescence signal at 710 nm for **2** corresponds to the energy of the triplet at 40 kcal/mol.

**Triplet-Triplet Spectra and Extinction Coefficients.** Excitation of the fullerenes at 355 nm generates the singlet state, which undergoes intersystem crossing to the triplet state. The transient absorption of the triplet state can be observed using flash photolysis in the microsecond range. For the mono-, bis-, and tris-substituted adducts, the peak of maximum absorption gradually shifts to the blue, while for the more derivatized fullerenes, the pattern becomes more complicated. The hexa-adduct **6** does not present the common fullerene derivative bands at  $\sim 700$  nm and most likely has a completely different triplet structure.

Triplet-triplet extinction coefficients ( $\Delta\epsilon_{T-T}$ ) were calculated using the energy-transfer method.<sup>26</sup> Rubrene ( $\sim 2 \mu\text{M}$ ,  $E_T = 26$  kcal/mol)<sup>23</sup> was added to a sample of  $\text{C}_{60}$  or fullerene adduct in toluene. Selective excitation of the fullerene at 355 nm and subsequent intersystem crossing cause formation of the triplet. The energy is then transferred to rubrene (Scheme 3).

### SCHEME 3



Quenching of the fullerene triplet and formation of the rubrene triplet can be easily monitored by flash photolysis. The fullerene triplet was observed at its  $T-T$   $\lambda_{\text{max}}$ , and the rubrene triplet is observed at 490 nm.<sup>27</sup> The primary reference is  $\text{C}_{60}$  ( $\Delta\epsilon_{T-T} = 20\,200 \text{ M}^{-1} \text{ cm}^{-1}$ ).<sup>28</sup> The data gathered were corrected for incomplete energy transfer using eq 1 and for fast decay of the rubrene triplet using eq 2. The values from these equations were used in eq 3 to calculate the final values of  $\Delta\epsilon_{T-T}$ .

$$P_{\text{tr}} = k_{\text{et}}[\text{Rub}] / (k_{\text{et}}[\text{Rub}] + k_D) \quad (1)$$

$$\Delta\text{OD}_{\text{Rub}} = \Delta\text{OD}_{\text{Rub}}(t_{\text{max}}) e^{k_A t_{\text{max}}} \quad (2)$$

$$\Delta\epsilon(T-T)_{\text{Rub}} = \Delta\epsilon(T-T)_S \left( \frac{\Delta\text{OD}_{\text{Rub}}}{\Delta\text{OD}_S} \right) \left( \frac{1}{P_{\text{tr}}} \right) \quad (3)$$

**Triplet Quantum Yields.** Quantum yields for the triplet state of the fullerene derivatives were calculated using the comparative technique of Bensasson et al.<sup>29</sup> The intensities of the



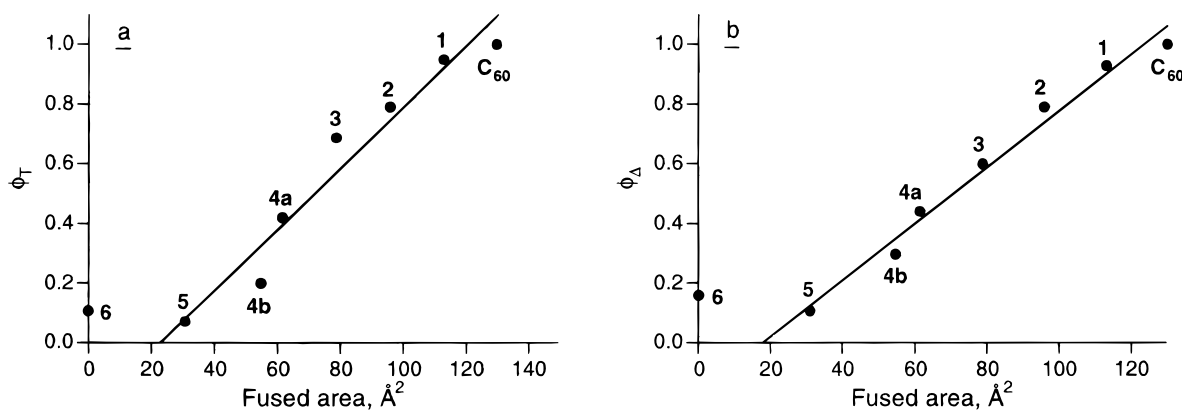
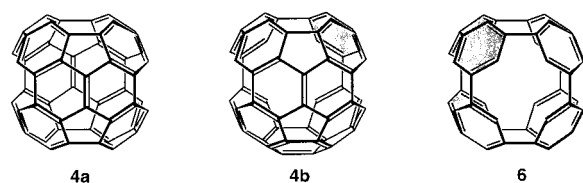


**Figure 5.** Correlation of the triplet (a) and singlet oxygen (b) quantum yields with the fused area of the fullerene core.

**TABLE 3: Singlet Oxygen Quantum Yields ( $\Phi_{\Delta}$ ) of Fullerene Adducts in Toluene**

compound	$C_{60}$	1	2	3	4a	4b	5	6
$\phi_{\Delta}$	1	0.93	0.79	0.60	0.44	0.30	0.11	0.16

#### SCHEME 4



#### SCHEME 5



transient absorption signals from optically matched samples of fullerene adduct and  $C_{60}$  were compared using eq 4 where  $\phi_T$

$$\Delta\epsilon_{T-T}(S) \phi_T(S) = \Delta\epsilon_{T-T}(C_{60}) \phi_T(C_{60}) \quad (4)$$

$= 1$  and  $\Delta\epsilon_{T-T} = 20\,200 \text{ M}^{-1} \text{ cm}^{-1}$  for  $C_{60}$ , and the value of  $\Delta\epsilon_{T-T}$  is taken from the previous experiment for the fullerene adducts.<sup>15,29</sup> Results for both triplet–triplet extinction coefficients and triplet quantum yields are summarized in Table 2.

As in the case of the triplet energies, triplet quantum yields show a strong correlation with the structure of the fullerene core (Figure 5a). These values of  $\phi_T$  are calculated indirectly from the previous measurements of  $\Delta\epsilon_{T-T}$  and therefore have an inherently large error. However, they correspond well with the values for singlet oxygen quantum yield calculated in the next section, which provide a lower limit for the triplet quantum yields.

**Singlet Oxygen Quantum Yields.** The production of  $^1O_2$  by the fullerene adduct was evaluated from the phosphorescence of singlet oxygen at 1268 nm.<sup>30</sup> For each compound, four samples with different absorbances ( $A = 0.05\text{--}0.4$ ) were prepared and the intensity of singlet oxygen emission measured. The observed intensity is linear with the absorptivity of the samples, and the ratio of the slopes of the plots is proportional to the ratio of singlet oxygen quantum yields.  $C_{60}$  was used as

the primary reference ( $\phi_{\Delta} = 1$ ). The results are summarized in Table 3. As mentioned previously, these results set a lower limit for the triplet quantum yield and are significantly more reliable than those calculated through the use of energy transfer and comparative experiments.

By comparison of the values obtained for the triplet and  $^1O_2$  quantum yields, it seems reasonable to conclude that the fraction of triplet that generates singlet oxygen,  $S_{\Delta} = \phi_{\Delta}/\phi_T$ , is roughly unity for all fullerene derivatives studied. Singlet oxygen quantum yields show the best correlation with the total conjugated fused area in the fullerene core (Figure 5b), compared to  $E_T$  and  $\phi_T$ . Remarkably, **4a** generates almost 50% more singlet oxygen than **4b**, even though they both have the same number of substituents. This difference shows the dramatic effect of the position of the substituents on the photophysical properties of fullerene adducts. According to Scheme 4, this difference can be rationalized in terms of smaller fused areas. Because of the orientation of the adduct moieties, **4b** presents two isolated phenyl groups (shaded in Scheme 4), whereas **4a** has two equal nearly half-fullerene fused structures. This feature is especially important in **6**. This compound has no fused area, and all its phenyl rings are connected to other phenyl rings by single bonds. The final result is a linked biphenyl macrostructure with special characteristics. In **6** the phenyl rings are forced to be almost coplanar, whereas in biphenyl the two rings are twisted with a  $45^\circ$  dihedral angle, and therefore, little inter-ring conjugation is possible.<sup>13</sup> However, the spherical nature of the fullerene cage forces the linked biphenyl units to bend around the  $sp^2$  carbons that connect both rings with a  $35^\circ$  deviation from planarity, as shown in Scheme 5.<sup>31</sup> As a result, substantial conjugation occurs, as confirmed by the relatively long wavelength absorption. Furthermore, an additional source of conjugation can be attributed to the cyclopropane rings. It is well known that the bent bonds of cyclopropane exhibit some  $\pi$  character.<sup>17</sup> This phenomenon in fullerenes has been previously described.<sup>14d,32</sup> Conjugation between a cyclopropane-type bond and adjacent double bonds is maximum when they are coplanar,<sup>33</sup> as is the case in these adducts. It is not unreasonable then to suggest that the singlet oxygen quantum yield for **6** ( $\phi_{\Delta} = 0.16$ ) results from this conjugation involving the eight phenyl rings plus additional conjugation due to the cyclopropane rings.

As we examine adducts with fewer substituents, another phenomenon (building of the corannulene structure up to the pristine fullerene  $C_{60}$ ) becomes more important and dominates the overall properties of the triplet state and subsequently its singlet oxygen generation capabilities.

## Conclusions

The triplet states of a complete series of fullerene Bingel adducts have been studied. The perturbation of the  $\pi$  system of the fullerene causes the photophysical properties to change substantially. Triplet energies, triplet quantum yields, and singlet oxygen quantum yields show a very good correlation with the fused conjugated area in the fullerene core. Successive functionalization of  $\text{C}_{60}$  results in higher triplet energies and lower triplet and singlet oxygen quantum yields. The hexaadduct **6** shows a different behavior and does not follow the same pattern as the other derivatives. This can be attributed to the disappearance of the pyracylene substructure and the presence of the linked biphenyl cage and attached cyclopropane rings as the only source of conjugation beyond the phenyl rings. It has been reported that other hexaadducts possess very surprising photophysical characteristics,<sup>4,34</sup> and such compounds will be the subject of intensive study in the future.

**Acknowledgment.** We thank Professor Miguel Garcia-Garibay and Brent Johnson for their advice and aid in the acquisition of phosphorescence data. We are grateful to the National Science Foundation (CHE-97-03086, C.S.F.; CHE-9457693, Y.R.) for support.

## References and Notes

- Anderson, J. L.; An, Y. Z.; Rubin, Y.; Foote, C. S. *J. Am. Chem. Soc.* **1994**, *116*, 9763–9764.
- Ma, B.; Bunker, C. E.; Guduru, R.; Zhang, X.-F.; Sun, Y.-P. *J. Phys. Chem. A* **1997**, *101*, 5626–5632.
- Nakamura, Y.; Minowa, T.; Hayashida, Y.; Tobita, S.; Shizuka, H.; Nishimura, J. *J. Chem. Soc., Faraday Trans.* **1996**, *92*, 377–382.
- Coheur, P. F.; Cornil, J.; dos Santos, D. A.; Birkett, P. R.; Liévin, J.; Brédas, J. L.; Janot, J. M.; Seta, P.; Leach, S.; Walton, D. R. M.; Taylor, R.; Kroto, H. W.; Colin, R. *Proc. Electrochem. Soc.* **1998**, *98* (8), 1170–1185.
- Sun, Y.-P.; Lawson, G. E.; Riggs, J. E.; Ma, B.; Wang, N. X.; Moton, D. K. *J. Phys. Chem. A* **1998**, *102*, 5520–5528.
- Williams, R. M.; Zwier, J. M.; Verhoeven, J. W. *J. Am. Chem. Soc.* **1995**, *117*, 4093–4099.
- Williams, R. M.; Koeberg, M.; Lawson, J. M.; An, Y.-Z.; Rubin, Y.; Paddon-Row, M. N.; Verhoeven, J. W. *J. Org. Chem.* **1996**, *61*, 5055–5062.
- Guldi, D. M.; Hungerbühler, H.; Asmus, K. D. *J. Phys. Chem.* **1995**, *99*, 9380–9385.
- Guldi, D. M.; Asmus, K. D. *J. Phys. Chem. A* **1997**, *101*, 1472–1481.
- Diederich, F.; Thilgen, C. *Science* **1996**, *271*, 317–323.
- Prato, M.; Maggini, M. *Acc. Chem. Res.* **1998**, *31*, 519–526.
- Hirsch, A. *Top. Curr. Chem.* **1999**, *199*, 1–65.
- Boudon, C.; Gisselbrecht, J. P.; Gross, M.; Isaacs, L.; Anderson, H. L.; Faust, R.; Diederich, F. *Helv. Chim. Acta* **1995**, *78*, 1334–1344.
- For related work on multiply cyclopropanated  $\text{C}_{60}$ , see the following. (a) Hirsch, A.; Lamparth, I.; Grösser, T.; Karfunkel, H. R. *J. Am. Chem. Soc.* **1994**, *116*, 9385–9386. (b) Hirsch, A.; Lamparth, I.; Karfunkel, H. R. *Angew. Chem., Int. Ed. Engl.* **1994**, *33*, 437–438. (c) Diederich, F.; Isaacs, L.; Philp, D. *Chem. Soc. Rev.* **1994**, *23*, 243–255. (d) Cardullo, F.; Seiler, P.; Isaacs, L.; Nierengarten, J. F.; Haldimann, R. F.; Diederich, F.; Mordasini-Denti, T.; Thiel, W.; Boudon, C.; Gisselbrecht, J. P.; Gross, M. *Helv. Chim. Acta* **1997**, *80*, 343–371. (e) Pasimeni, L.; Hirsch, A.; Lamparth, I.; Herzog, A.; Maggini, M.; Prato, M.; Corvaja, C.; Scorrano, G. *J. Am. Chem. Soc.* **1997**, *119*, 12896–12901. (f) Pasimeni, L.; Hirsch, A.; Lamparth, I.; Maggini, M.; Prato, M. *J. Am. Chem. Soc.* **1997**, *119*, 12902–12905. (g) Diederich, F.; Kessinger, R. *Acc. Chem. Res.* **1999**, *32*, 537–545.
- Foote, C. S. *Electron Transfer I*; Mattay, J., Ed.; Topics in Current Chemistry 169; Springer-Verlag: New York, 1994; pp 347–363.
- Hamano, T.; Okuda, K.; Mashino, T.; Hirobe, M.; Arakane, K.; Ryu, A.; Mashiko, S.; Nagano, T. *Chem. Commun.* **1997**, 21–22.
- Staley, S. W. *J. Am. Chem. Soc.* **1967**, *89*, 1532–1533.
- Qian, W.; Rubin, Y. *Angew. Chem.*, in press.
- The MER Corp., 7960 S. Kolb Road, Tucson, AZ 85706.
- Garcia-Garibay, M. A.; Gamarnik, A.; Bise, R.; Pang, L.; Jenks, W. S. *J. Am. Chem. Soc.* **1995**, *117*, 10264–10275.
- Zeng, Y.; Biczok, L.; Linschitz, H. *J. Phys. Chem.* **1992**, *96*, 5237–5239.
- Arbogast, J. W.; Foote, C. S. *J. Am. Chem. Soc.* **1991**, *113*, 8886–8889.
- Murov, S. L.; Carmichael, I.; Hug, G. L. *Handbook of Photochemistry*; Marcel Dekker: New York, 1993.
- Herkstroeter, W. G. *J. Am. Chem. Soc.* **1975**, *97*, 4161–4167.
- Arbogast, J. W.; Foote, C. S.; Kao, M. *J. Am. Chem. Soc.* **1992**, *114*, 2277–2279.
- Carmichael, I.; Hug, G. L. *J. Phys. Chem. Ref. Data* **1986**, *15*, 1–250.
- Malkin, Y. N.; Pirogov, O.; Kuzmin, V. A. *J. Photochem.* **1984**, *26*, 193–202.
- Bensasson, R. V.; Hill, T.; Lambert, C.; Land, E. J.; Leach, S.; Truscott, T. G. *Chem. Phys. Lett.* **1993**, *201*, 326–335.
- Bensasson, R. V.; Bienvenue, E.; Janot, J. M.; Leach, S.; Seta, P.; Schuster, D. I.; Wilson, S. R.; Zhao, H. *Chem. Phys. Lett.* **1995**, *245*, 566–570.
- Foote, C. S.; Clennan, E. L. *Active Oxygen in Chemistry*; Foote, C. S., Valentine, J. S., Greenberg, A., Liebman, J. F., Eds.; Blackie Academic and Professional: New York, 1995.
- Deviation from planarity was calculated by molecular modeling using MacroModel 6.0 and Spartan 5.0. The geometry of **6** was optimized using a MM3 force field.
- Saunders, M.; Cross, R. J.; Jiménez-Vázquez, H. A.; Shimshi, R.; Khong, A. *Science* **1996**, *271*, 1693–1697.
- Jorgenson, M. J.; Leung, T. *J. Am. Chem. Soc.* **1968**, *90*, 3769–3774.
- Schick, G.; Levitus, M.; Kvetko, L.; Johnson, B. A.; Lamparth, I.; Lunkwitz, R.; Ma, B.; Khan, S. I.; Garcia-Garibay, M. A.; Rubin, Y. *J. Am. Chem. Soc.* **1999**, *121*, 3246–3247.